

Deep Neural Network-Based Detector for Single-Carrier Index Modulation NOMA

Toan Gian, Vu-Duc Ngo, Tien-Hoa Nguyen, Trung Tan Nguyen, and Thien Van Luong

Abstract—In this paper, a deep neural network (DNN)-based detector for an uplink single-carrier index modulation non-orthogonal multiple access (SC-IM-NOMA) system is proposed, where SC-IM-NOMA allows users to use the same set of sub-carriers for transmitting their data modulated by the sub-carrier index modulation technique. More particularly, users of SC-IM-NOMA simultaneously transmit their SC-IM data at different power levels which are then exploited by their receivers to perform successive interference cancellation (SIC) multi-user detection. The existing detectors designed for SC-IM-NOMA, such as the joint maximum-likelihood (JML) detector and the maximum likelihood SIC-based (ML-SIC) detector, suffer from high computational complexity. To address this issue, we propose a DNN-based detector whose structure relies on the model-based SIC for jointly detecting both M -ary symbols and index bits of all users after trained with sufficient simulated data. The simulation results demonstrate that the proposed DNN-based detector attains near-optimal error performance and significantly reduced runtime complexity in comparison with the existing hand-crafted detectors.

Index Terms—Non-orthogonal multiple access, NOMA, uplink, successive interference cancellation, SIC, deep learning, DeepSIC-IM, DNN, bit error rate, runtime complexity.

I. INTRODUCTION

Wireless technologies have been anticipated to move from the conventional orthogonal to non-orthogonal solutions to meet requirements of future wireless networks, such as, ubiquitous coverage, high data rate, low latency, high transmission reliability and scalability [1], [2]. In particular, using non-orthogonal multiple access (NOMA) techniques, different users can simultaneously share the same wireless resources for supporting a massive number of devices. Moreover, in NOMA, multiple users can transmit data at different power levels over the same radio resources, which facilitates successive interference cancellation (SIC) to be effective for detecting the desired signal. Thus, NOMA is a potential solution to improve spectrum efficiency, reduce latency and provide high reliability, and facilitate massive connection compared to the conventional orthogonal multiple access (OMA) [3].

Index modulation (IM) has been known as an effective solution to provide trade-off among transmission reliability,

spectrum and energy efficiency. In IM-based systems, information bits are implicitly encoded in indices of several facilities such as antennas, subcarriers, and spreading codes [4]. For example, using the indices of active sub-carriers as an additional domain to the traditional modulated symbols, the orthogonal frequency division multiplexing with IM (OFDM-IM) was proposed in [3], which significantly improves the error performance compared with conventional OFDM. Since then, many efforts have been made in order further improve either the error performance or spectral efficiency of OFDM-IM, as can be found in [4]–[7]. Moreover, the bit error rate (BER), symbol error probability (SEP), and outage probability of OFDM-IM using different detection types over different channel state information (CSI) conditions were intensively analyzed in [8]–[11], which provide helpful insights into its error performance as well as impacts of CSI uncertainty.

Recently, OFDM-IM has been applied to multi-user communications, particularly to massive machine-type communications (mMTC), which require massive connectivity with highly power-efficient transmissions [12]. For example, aiming at reducing peak to average power ratio (PAPR) inherited from the OFDM framework, the single-carrier frequency division multiple access (SC-FDMA) was combined with sub-carrier index modulation in a NOMA manner in [13]. The resultant scheme called SC-IM-NOMA was demonstrated to achieve higher energy efficiency and better BER performance than its single-carrier IM-based OMA counterparts (called SC-IM) proposed in [12], [14]. Note that the SC-IM schemes proposed in [12] and [14] are based on OMA, in which each user is allocated a dedicated set of subcarriers for employing SC-IM transmissions to achieve better BER performance than conventional SC-FDMA. Yet, SC-IM is not spectrum-efficient compared with SC-IM-NOMA in [13], which allows different users to use the same set of sub-carriers for SC-IM transmissions. As a result, SC-IM-NOMA is particularly appropriate for uplink mMTC systems. However, SC-IM-NOMA, the joint maximum-likelihood (JML) detector and the combination of maximum likelihood (ML) and SIC methods (ML-SIC), suffers from high detection complexity compared to both SC-FDMA and SC-IM receivers. Therefore, our paper appears to tackle this fundamental issue.

In this paper, we propose a deep neural network (DNN)-based detector for the uplink SC-IM-NOMA system, called DeepSIC-IM, which can significantly reduce the complexity, while achieving near-optimal BER performance compared with the existing hand-designed detectors. Consider two uplink

Toan Gian, Vu-Duc Ngo, and Tien-Hoa Nguyen are with the School of Electrical and Electronics Engineering, Hanoi University of Science and Technology, Hanoi, Vietnam. (e-mail: toandinh7176@gmail.com, {hoa.nguyentien,duc.ngovu}@hust.edu.vn).

Trung Tan Nguyen is with the Faculty of Radio-Electronics, Le Quy Don Technical University, Ha Noi 11355, Vietnam (e-mail: trungtan-nguyen@mta.edu.vn).

Thien Van Luong is with the Faculty of Computer Science, Phenikaa University, Hanoi 12116, Vietnam (e-mail: thien.luongvan@phenikaa-uni.edu.vn).

NOMA users, we design a DNN structure for DeepSIC-IM, that relies on the model-based SIC procedure for jointly detecting both M -ary symbols and index bits of both users. More particularly, the proposed DeepSIC-IM consists of two different DNNs, each is dedicated for detecting the signal of the corresponding user when fed with the received signal and the output of the interfering users. Using simulated dataset, DeepSIC-IM is trained offline to jointly minimize the BERs of both users. Then, the trained model can be deployed in an on-line manner with very low runtime. For this, simulation results are provided to demonstrate that our DeepSIC-IM detector provides near-optimal BER performance at remarkably lower runtime complexity than the existing hand-crafted detectors.

We note that deep learning (DL) or DNN techniques have been widely exploited for enhancing the performance of wireless communication systems. For example, in [15], a DL-based detector was proposed for OFDM-IM, achieving low runtime complexity and near-optimal error performance. The channel estimation and signal detection in OFDM were performed based on DNN in [16]. An application of DL for downlink NOMA receivers was presented in [17], which, however, only considers the conventional M -ary modulation, without any index modulation. A number of other DL applications for designing the reliable and low-complexity transceiver of wireless systems can be found in [18]–[21].

The rest of this paper is organized as follows. Section II describes the system model of SC-IM-NOMA and its existing detection. Section III presents the proposed DeepSIC-IM structure and its corresponding training process. Section IV provides simulation results and discussion for BER and runtime complexity. Finally, Section V concludes the paper.

II. SYSTEM MODEL

Consider an uplink scenario where two users ($L = 2$), $l \in (1, 2)$, transmit data bits to the base station (BS) across the resource block (RB). Gains of channel user 1 to BS and user 2 to BS are represented as $|\mathbf{h}_1|$ and $|\mathbf{h}_2|$, respectively. Both of users transmit SC-IM-based signals to BS with power allocation coefficients of P_1 and P_2 , respectively, where $P_1 > P_2$. Each data block takes b bits from each of L users. Additionally, N and K stand for the total number of allotted and active subcarriers, respectively. Each SC-IM block transmits a b -bit stream and bits determine the set of M -ary modulated symbols that will be conveyed by K active subcarriers. In this paper, all users use the same N , K and M -ary modulation technique. Thus, $b = b^{ind} + b^{sym} = \lceil \log_2(N, K) \rceil + K \log_2(M)$ is the total number of bits transmitted by the l -th user in the SC-IM block [14], [12]. In the IM subblock, the l -th user's initial bits are divided into two parts. The first $b^{ind} = \log_2(N, K)$ bits are to select K active indices using either the combinatorial method or the look-up table [3]. The remaining $b^{sym} = K \log_2(M)$ bits are mapped to transmitted M -ary amplitude/phase modulated (APM) symbols. For example (as Fig. 1) with $(N, K, M) = (4, 2, 4)$, the transmitted signal vector, $\mathbf{x}_l = [x_l^1 0 0 x_l^2]^T$, is made up by symbols from an M -point constellation and zeros associated with the inactive

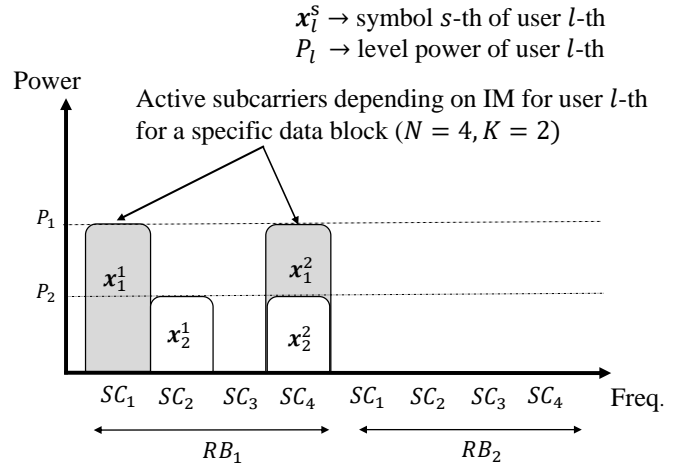


Fig. 1. Sub-carrier and power allocation of SC-IM-NOMA.

subcarriers, where x_l^s stands for the s -th symbol of the l -th user, $l = 1, 2$. The model can serve a certain number of users since SC-IM allocates a set of subcarriers to each user. Fig. 1 depicts a sample SC-IM-NOMA resource mapping for the scenario of two users. Both of users transmit data over the same RB using NOMA at distinct power levels.

The received signal at the BS over N subcarriers can be represented by

$$\mathbf{y} = \sum_{l=1}^L \sqrt{P_l} \mathbf{h}_l \odot \mathbf{x}_l + \mathbf{w}, \quad (1)$$

where \odot stands for the element-wise multiplication, $\mathbf{y} = [y(1), \dots, y(N)]^T$, $\mathbf{h}_l = [h_l(1), \dots, h_l(N)]^T$ is the channel vector, $\mathbf{x}_l = [x_l(1), \dots, x_l(N)]^T$ and $\mathbf{w} = [w_1, \dots, w_N]^T$ is the additive white Gaussian noise (AWGN) vector, P_l is the power for the l -th user.

In order to recover transmitted signal, the JML detector and ML-SIC detector [13] can be employed, which are described in the following.

1) *JML detector*: The JML detector performs an exhaustive search to simultaneously recover the transmitted vector \mathbf{x}_l for all l -th users. Consider the scenario of two users, both transmitted vectors \mathbf{x}_1 and \mathbf{x}_2 are recovered simultaneously as follow:

$$\{\hat{\mathbf{x}}_l\}_{l=1,2} = \arg \min_{\mathbf{x}_{l=1,2} \in \delta} \left\| \mathbf{y} - \sqrt{P_1} \mathbf{h}_1 \odot \mathbf{x}_1 - \sqrt{P_2} \mathbf{h}_2 \odot \mathbf{x}_2 \right\|, \quad (2)$$

where JML checks \mathbf{y} for all possible combinations of transmit vectors of users, which is denoted by δ . This detector can provide the optimal performance at the expense of high computational complexity, thus, it can be used as a benchmark when designing any low complexity receiver.

2) *ML-SIC detector*: Based on this, the SIC-ML detector of user l -th operates in the following iterative fashion. In the case of 2 users, user 1, which is allocated more power, will detect its own signal first by treating the interference from

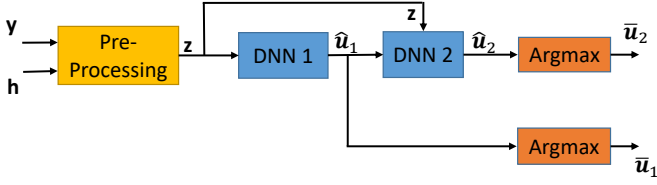


Fig. 2. The proposed DeepSIC-IM DNN structure.

TABLE I
PARAMETERS OF DNN 1 AND DNN 2 WITH $(N, K, M) = (4, 1, 4)$

Parameter	DNN 1	DNN 2
Input size	$2N + (l-1)2^b = 8$	$2N + (l-1)2^b = 24$
Output size	$2^b = 16$	$2^b = 16$
FC layer	3	3
Hidden Nodes	32-64	128-256

the user 2 as the noise. Using the ML criterion, the estimated signal of user 1 is determined by

$$\hat{\mathbf{x}}_1 = \arg \min_{\mathbf{x}_1 \in \delta} \left\| \mathbf{y} - \sqrt{P_1} \mathbf{h}_1 \odot \mathbf{x}_1 \right\|. \quad (3)$$

Then, the contribution of user 1 to \mathbf{y} is eliminated for decoding the signal of user 2. Explicitly, the symbol of user 2 is recovered using the ML estimate in which the interfering signal of user 1 is estimated by $\hat{\mathbf{x}}_1$, resulting in

$$\hat{\mathbf{x}}_2 = \arg \min_{\mathbf{x}_2 \in \delta} \left\| \left(\mathbf{y} - \sqrt{P_1} \mathbf{h}_1 \odot \hat{\mathbf{x}}_1 \right) - \sqrt{P_2} \mathbf{h}_2 \odot \mathbf{x}_2 \right\|. \quad (4)$$

From the formula (2), (3) and (4), the complexity of the conventional detectors mentioned above would increase, particularly when having more uplink NOMA users as well as when the SC-IM-NOMA parameters increase. Motivated by this issue, we propose a DL-based detector to detect transmitted signals with competitive performance and low complexity compared to these ML-based detectors.

III. PROPOSED DEEPSIC-IM DETECTOR

In this section, the structure of the proposed DeepSIC-IM detector and its training procedure are presented.

A. Structure of proposed DeepSIC-IM

The structure of DeepSIC-IM is illustrated in Fig. 2. Assume that the channel state information (CSI) is perfectly known at the receiver and considered as input of the decoder, along with the received signal \mathbf{y} . Hence, the well-known zero-forcing (ZF) equalizer is employed to get an equalized received signal vector as $\bar{\mathbf{y}} = \mathbf{y} \odot \mathbf{h}_1^{-1}$. Particularly, the complex vectors $\bar{\mathbf{y}}_R$ and $\bar{\mathbf{y}}_I$ are transformed into an $2N$ -dimensional real vector $\mathbf{z} = [\bar{\mathbf{y}}_R, \bar{\mathbf{y}}_I]$, as shown in Fig. 2, where $\bar{\mathbf{y}}_R$, $\bar{\mathbf{y}}_I$ are real and imaginary parts of $\bar{\mathbf{y}}$.

The input of the l -th DNN block includes both \mathbf{z} and the output of the previous $l-1$ DNN blocks, namely \mathbf{s}_l . More specifically, those elements are concatenated to form an input vector of the size $[2N + (l-1)2^b]$. Due to the complexity of each signal being different (the signal detection for l -th user will be more difficult than that for $(l-1)$ -th user), each DNN to detect each signal will have a different number of nodes, as shown in Table I.

The proposed decoder of each user has three nonlinear FC layers. At the hidden layer, either the rectifier linear unit (Relu), $f_{\text{Relu}}(x) = \max(0, x)$, or the hyperbolic tangent (Tanh) function, $f_{\text{Tanh}}(x) = \frac{1-e^{-2x}}{1+e^{-2x}}$, can be used as the activation function. The decoder generates an output probability vector $\hat{\mathbf{u}}_l$ with the Softmax layer as the output layer. The output vector $\hat{\mathbf{u}}_l$ of each DNN with size $[2^b]$ can be given by

$$\hat{\mathbf{u}}_l = f_{\text{Softmax}}(\mathbf{W}_3 f_{\text{Relu}}(\mathbf{W}_2 f_{\text{Relu}}(\mathbf{W}_1 \mathbf{s}_l + \mathbf{b}_1) + \mathbf{b}_2) + \mathbf{b}_3), \quad (5)$$

where \mathbf{W}_1 , \mathbf{b}_1 , \mathbf{W}_2 , \mathbf{b}_2 and \mathbf{W}_3 , \mathbf{b}_3 denote the weights and biases of the first, second and third FC layers, respectively, \mathbf{s}_l is the input vector of the l -th DNN, which is represented by $\mathbf{s}_l = [\mathbf{z}, \hat{\mathbf{u}}_1, \dots, \hat{\mathbf{u}}_{l-1}]$. Finally, we get the vector $\bar{\mathbf{u}}_l$ based on the largest entry of $\hat{\mathbf{u}}_l$. Then, the information prediction will be calculated.

Crucial points of the proposed scheme structure can be described as follows. First, the length of input and output of DeepSIC-IM is determined by system parameters such as N , K and M . This will make the complexity of the proposed scheme highly dependent on each of the three aforementioned indicators. Intuitively, when the number of transmitted b -bit increases, we need a number of nodes large enough to guarantee a predetermined performance. Therefore, the number of nodes of the l -th DNN (denoted by \mathcal{O}_l) must be carefully chosen to obtain the desired performance for each system configuration. The value of \mathcal{O}_l must be sufficiently large to ensure a predetermined performance. In addition, we can attain a promising trade-off between the detection accuracy and the model complexity by adjusting value of \mathcal{O}_l .

B. Training Procedure

Before implementing the proposed DeepSIC-IM technique, the DNN model with the collected data from simulation need to be trained. Initially, various b -bit sequences will be randomly created for L users and transformed into the matching vector \mathbf{x}_l . The one-hot vectors \mathbf{u}_l are generated first to create L sets of one-hot labels for L users, while noise vectors are randomly generated. At the receiver, \mathbf{y} and \mathbf{h}_1 are pre-processed to obtain the vector \mathbf{z} , which is then combined with the output of the previous $l-1$ DNN blocks to provide the input for the l -th DNN block \mathbf{s}_l . The mean square error (MSE) cost function which is adopted to measure the difference between the estimation vector $\hat{\mathbf{u}}_l$ and its true value vector \mathbf{u}_l , as follows:

$$\mathcal{L}(\mathbf{u}_l, \hat{\mathbf{u}}_l; \theta_l) = \sum_{l=1}^L \frac{1}{b} \|\mathbf{u}_l - \hat{\mathbf{u}}_l\|^2, \quad (6)$$

where $\theta_l = \{\mathbf{W}_i, \mathbf{b}_i\}_{i=1,2,3}$ are the weights and biases of the l -th DNN user model, \mathbf{u}_l is the collection of one hot vector corresponding to b bits trained offline and $\hat{\mathbf{u}}_l$ is the output vector of the l -th DNN. Model parameters are updated for the batches randomly picked up from data samples, using the stochastic gradient descent (SGD) algorithm as follows

$$\theta^+ := \theta - \eta \nabla \mathcal{L}(\mathbf{u}_l, \hat{\mathbf{u}}_l; \theta), \quad (7)$$

TABLE II
A SUMMARY OF SIMULATION PARAMETERS

Parameter	Value
Number of users L	2
Parameters of index modulation (N, K, M)	4,1,4
Gains of channel $\mathbf{h}_1, \mathbf{h}_2$	[2, 2, 2, 2], [1, 1, 1, 1]
Power allocation coefficient P_1, P_2	2,1
Hidden nodes of DNN 1	32-64
Hidden nodes of DNN 2	128-256
Activation for hidden layers of DNN 1	Tanh
Activation for output layers of DNN 1, 2	Softmax
Activation for hidden layers of DNN 2	Relu
Training SNR λ_{train}	16, 18, 20, 22, 24 dB
Learning rate η	0.001
Batch size	200
Number of training epochs	500
Training data size	2×10^6
Testing data size	10^6
Optimizer	Adam [22]

where η is learning rate. In our training, we use the adaptive moment estimation (Adam) optimizer, a sophisticated updating technique built on SGD. The signal to noise ratio (SNR) training (denoted as λ_{train}), which has a significant impact on the performance of the training model, will be chosen to suit the model as closely as possible. For instance, if λ_{train} train is too small, the training will not account for the influence of noise, which will result in poor generalization of the trained model. Choosing a suitable λ_{train} for achieving the desired performance will be presented in detail in the simulations.

IV. SIMULATION RESULTS

This section presents simulation results to demonstrate the performance of our DeepSIC-IM compared to the existing schemes, including JML and ML-SIC detectors, in terms of both BER and runtime complexity.

A. Parameter Setting

In Table II, we summarize the SC-IM-NOMA system parameters as well as the DNN model parameters, which are used for conducting simulations in this section. For example, we train our DeepSIC-IM with 500 epochs, each contains 10^4 samples, where the batch size is 200 samples. During training, data samples are randomly generated for each batch. Therefore, we have a total of 2×10^6 different data samples for training, while the testing size is 10^6 samples. The learning rate η is set to be 0.001.

We note that in this work we only consider fixed channels for both users, as shown in Table II. For varying or random fading channels, we may have to use some advanced training techniques, such as feed-forward error correction (FEC)-aided online labeling [17]. We consider such the extension as our future work. Furthermore, throughout extensive experiments, we discovered that user 1 would prefer the Tanh activation function, while user 2 would prefer the Relu activation function, for better BER performance, as shown in Table II.

B. BER Performance

The BER performance of user 1 and user 2 using the proposed DeepSIC-IM trained at various training SNRs is

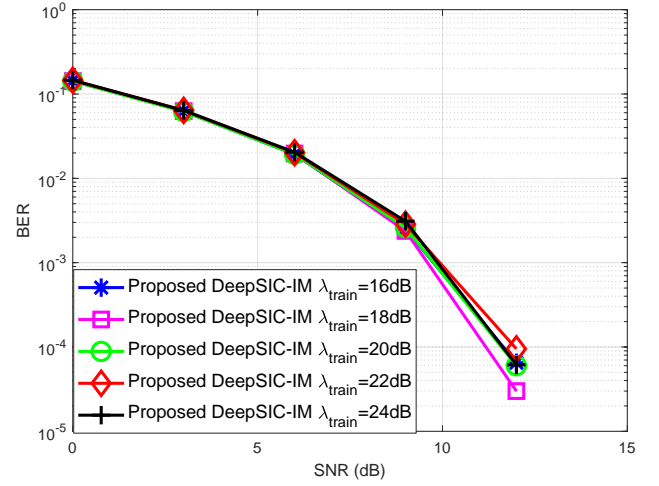


Fig. 3. BER performance of DeepSIC-IM for user 1 trained at various training SNRs λ_{train} . The training setting is described in Table II.

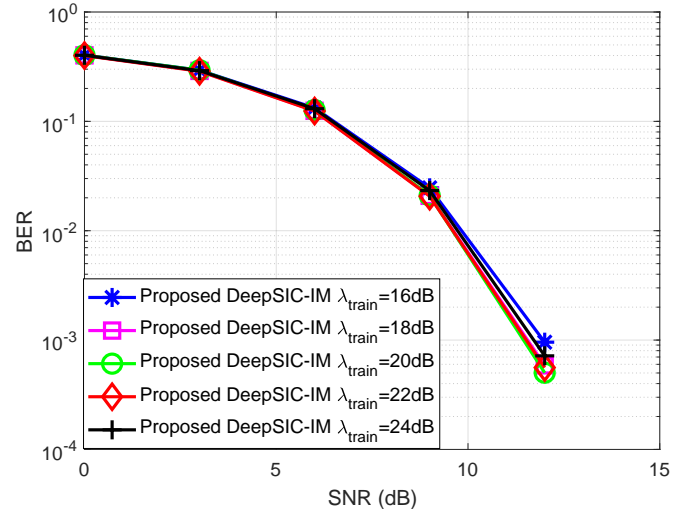


Fig. 4. BER performance of DeepSIC-IM for user 2 trained at various training SNRs λ_{train} . The training setting is described in Table II.

illustrated in Fig. 3 and Fig. 4, respectively. It is shown from both figures that the BER performance achieved by DeepSIC-IM for both users varies with respect to the training SNR, especially at high testing SNRs. It is also observed that our proposed DeepSIC-IM tends to achieve the best BER for the two users when the training SNR is between 18 and 20 dB. Therefore, in the following, we will use a training SNR of 18 dB for training DeepSIC-IM to compare with the baseline.

Fig. 5 compares the BER performance among the proposed DeepSIC-IM detector, JML and ML-SIC detector, where both users are considered, and our scheme is trained at 18 dB. It is shown from Fig. 5 that the proposed learning detector attains BER performance very close to that of the JML and ML-SIC detectors. For example, at the BER of 10^{-2} , the SNR gap between the proposed detector, JML and ML-SIC is negligible with less than 0.4 dB and 0.3 dB, respectively, while our detector requires much lower runtime complexity

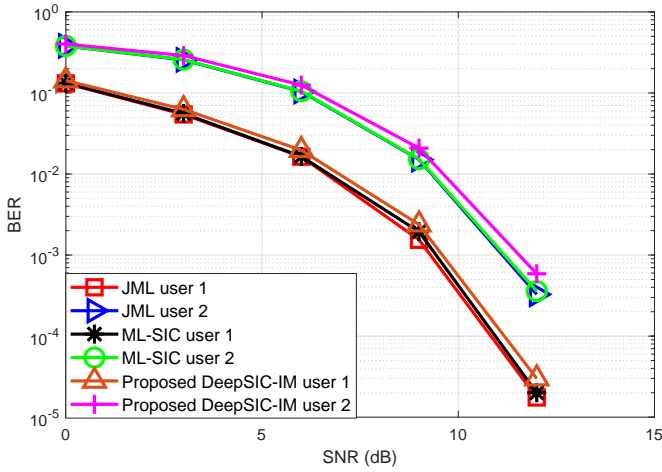


Fig. 5. BER comparison between the proposed DeepSIC-IM and baselines with training SNR $\lambda_{train} = 18\text{dB}$. The training setting is described in Table II.

than its counterpart, as shown in the following subsection.

C. Runtime Complexity

We now measure the runtime for detecting each sample of the proposed DeepSIC-IM, JML and ML-SIC detectors. In particular, we convert the DeepSIC-IM model that was trained using the Tensorflow library to MATLAB. To ensure a fair comparison, the JML and ML-SIC detectors are also run on MATLAB on the same computer. The obtained complexity for the three detectors measured in seconds is compared in Table III. It is shown from this table that the proposed learning detector demands much less runtime than both the JML and ML-SIC detectors. More particularly, the runtime of our DeepSIC-IM is 7 and 3 times less than that of the JML and ML-SIC, respectively, which clearly validates the advantage of the proposed detector in terms of runtime complexity.

TABLE III
COMPLEXITY COMPARISON AMONG DEEPSIC-IM, JML AND ML-SIC

(N, K, M)	JML	ML-SIC	DeepSIC-IM
(4,1,4)	7.65×10^{-4}	3.31×10^{-4}	1.14×10^{-4}

V. CONCLUSIONS

In this paper, we proposed the DeepSIC-IM detector for the SC-IM-NOMA system. In particular, we designed a novel DNN structure for SC-IM-NOMA that includes several DNN blocks, each used for detecting the transmitted signal of the corresponding user, where its input data is made up of the pre-processed received signal and the output of the interfering users. Once trained with simulated dataset, our proposed method can be deployed for detecting data bits in an online manner with very low runtime. Our simulation results demonstrated that the proposed DeepSIC-IM detector achieves near-optimal BER performance at remarkably lower runtime complexity compared to the existing ML-based detectors. Although we only consider two uplink NOMA users in this work, the extension of DeepIM-SIC for more users is straightforward. In the future, we plan to extend the proposed

DeepSIC-IM to time-varying channels, where the channel coding-aided online training technique in [17] is helpful.

REFERENCES

- [1] Z. Ding, X. Lei, G. K. Karagiannidis, R. Schober, J. Yuan, and V. K. Bhargava, "A survey on non-orthogonal multiple access for 5G networks: Research challenges and future trends," *IEEE J. Sel. Areas Commun.*, vol. 35, no. 10, pp. 2181–2195, 2017.
- [2] Y. Liu, Z. Qin, M. El-Kashlan, Z. Ding, A. Nallanathan, and L. Hanzo, "Nonorthogonal multiple access for 5G and beyond," *Proc. IEEE*, vol. 105, no. 12, pp. 2347–2381, 2017.
- [3] E. Basar, U. Aygolu, E. Panayirci, and H. V. Poor, "Orthogonal frequency division multiplexing with index modulation," *IEEE Transactions on Signal Proc.*, vol. 61, no. 22, pp. 5536–5549, 2013.
- [4] T. V. Luong and Y. Ko, "Spread OFDM-IM with precoding matrix and low-complexity detection designs," *IEEE Trans. Veh. Technol.*, vol. 67, no. 12, pp. 11 619–11 626, Dec. 2018.
- [5] T. Mao, Z. Wang, Q. Wang, S. Chen, and L. Hanzo, "Dual-mode index modulation aided OFDM," *IEEE Access*, vol. 5, pp. 50–60, 2017.
- [6] T. V. Luong, Y. Ko, and J. Choi, "Repeated MCIC-OFDM with enhanced transmit diversity under CSI uncertainty," *IEEE Trans. Wireless Commun.*, vol. 17, no. 6, pp. 4079–4088, June 2018.
- [7] M. Wen, B. Ye, E. Basar, Q. Li, and F. Ji, "Enhanced orthogonal frequency division multiplexing with index modulation," *IEEE Trans. Wireless Commun.*, vol. 16, no. 7, pp. 4786–4801, 2017.
- [8] T. V. Luong and Y. Ko, "Impact of CSI uncertainty on MCIC-OFDM: Tight closed-form symbol error probability analysis," *IEEE Trans. Veh. Technol.*, vol. 67, no. 2, pp. 1272–1279, 2018.
- [9] T. V. Luong and Y. Ko, "The BER analysis of MRC-aided greedy detection for OFDM-IM in presence of uncertain CSI," *IEEE Wireless Commun. Lett.*, vol. 7, no. 4, pp. 566–569, Aug. 2018.
- [10] T. Van Luong and Y. Ko, "A tight bound on BER of MCIC-OFDM with greedy detection and imperfect CSI," *IEEE Commun. Lett.*, vol. 21, no. 12, pp. 2594–2597, 2017.
- [11] T. V. Luong and Y. Ko, "Symbol error outage performance analysis of MCIC-OFDM over complex TWDP fading," in *Proc. Eur. Wireless*, May 2017, pp. 1–5.
- [12] J. Manco-Vasquez, M. Chafii, and F. Bader, "Tailoring index-modulation for uplink IoT and M2M networks," in *2019 IEEE Wireless Commun. and Networking Conference (WCNC)*, 2019, pp. 1–6.
- [13] M. B. Shahab, S. J. Johnson, M. Shirvanmoghaddam, M. Chafii, E. Basar, and M. Dohler, "Index modulation aided uplink NOMA for massive machine type communications," *IEEE Wireless Commun. Lett.*, vol. 9, no. 12, pp. 2159–2162, 2020.
- [14] M. Chafii, F. Bader, and J. Palicot, "SC-FDMA with index modulation for M2M and IoT uplink applications," in *2018 IEEE Wireless Commun. and Networking Conference (WCNC)*, 2018, pp. 1–5.
- [15] T. V. Luong, Y. Ko, N. A. Vien, D. H. N. Nguyen, and M. Matthaiou, "Deep learning-based detector for OFDM-IM," *IEEE Wireless Commun. Lett.*, vol. 8, no. 4, pp. 1159–1162, 2019.
- [16] H. Ye, G. Y. Li, and B.-H. Juang, "Power of deep learning for channel estimation and signal detection in OFDM systems," *IEEE Wireless Commun. Lett.*, vol. 7, no. 1, pp. 114–117, 2018.
- [17] T. V. Luong, N. Shlezinger, C. Xu, T. M. Hoang, Y. C. Eldar, and L. Hanzo, "Deep learning based successive interference cancellation for the non-orthogonal downlink," *IEEE Trans. Veh. Technol.*, pp. 1–13, 2022.
- [18] T. Van Luong, Y. Ko, N. A. Vien, M. Matthaiou, and H. Q. Ngo, "Deep energy autoencoder for noncoherent multicarrier MU-SIMO systems," *IEEE Trans. Wireless Commun.*, vol. 19, no. 6, pp. 3952–3962, 2020.
- [19] C. Xu, T. Van Luong, L. Xiang, S. Sugiura, R. G. Maunder, L.-L. Yang, and L. Hanzo, "Turbo detection aided autoencoder for multi-carrier wireless systems: Integrating deep learning into channel coded systems," *IEEE Trans. Cogn. Commun. Netw.*, vol. 8, no. 2, pp. 600–614, 2022.
- [20] T. V. Luong, Y. Ko, M. Matthaiou, N. A. Vien, M. T. Le, and V. D. Ngo, "Deep learning-aided multicarrier systems," *IEEE Trans. Wireless Commun.*, vol. 20, no. 3, pp. 2109–2119, 2021.
- [21] T. Van Luong, X. Zhang, L. Xiang, T. M. Hoang, C. Xu, P. Petropoulos, and L. Hanzo, "Deep learning-aided optical IM/DD OFDM approaches the throughput of RF-OFDM," *IEEE J. Sel. Areas Commun.*, vol. 40, no. 1, pp. 212–226, 2022.
- [22] D. P. Kingma and J. Ba, "Adam: A method for stochastic optimization," *ICLR*, 2014.